ACADEMIA ROMÂNĂ
Revue Roumaine de Chimie
http://web.icf.ro/rrch/

Rev. Roum. Chim.,
2017, *62*(2), 131-138

FERROMAGNETIC MATERIALS OBTAINED THROUGH ULTRASONICATION. 1. MAGHEMITE/GOETHITE NANOCOMPOSITES

Razvan ROTARU,[a] Petrisor SAMOILA,[a] Nicoleta LUPU,[b] Marian GRIGORAS[b] and Valeria HARABAGIU[a*]

[a] "Petru Poni" Institute of Macromolecular Chemistry, 41A, Aleea Grigore Ghica Vodă, 700487 Iaşi, Roumania
[b] National Institute of Research and Development for Technical Physics, 47, Mangeron Boulevard, 700050, Iaşi, Roumania

Received July 26, 2016

Maghemite (γ-Fe_2O_3)/goethite (α-FeOOH) composite nanometric particles were prepared through an one-pot synthesis protocol, involving a chemical precipitation process performed under ultrasonication of iron sulfate in an aqueous basic solution. As proved by infrared spectroscopy, X-ray diffraction and electronic microscopy, the resulted ferromagnetic composite is composed of goethite acicular nanoparticles of average diameters less than 10 nm and lengths around or higher than 100 nm, surrounded by maghemite spherical nanoparticles with a diameter less than 100 nm. The composite nanoparticles functionalized with OH groups belonging to goethite showed also good magnetic properties specific to maghemite (the saturation magnetization is varying from 59.6 emu/g at room temperature to 75.5 emu/g at low temperature).

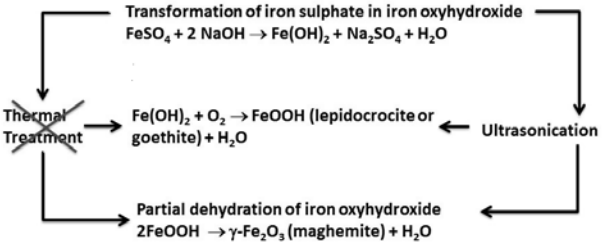

INTRODUCTION

Ferromagnetic monodispersed or polydispersed nanoparticles have attracted increasing attention due to their good biocompatibility, low toxicity, saturation magnetization higher than 60 emu/g, superparamagnetic properties and easy preparation process.[1,2] They have considerable potential for use in the biomedical industry, such as targeted drug delivery, hyperthermia treatment, cell separation, magnetic resonance imaging, immunoassays and the separation of biochemical products.[3-5] They are also useful for environmental processes, such as the treatment of wastewater.[6]

As a member of iron oxide family, maghemite (γ-Fe_2O_3) - having a spinel structure with two magnetically nonequivalent interpenetrating sublattices - exhibits a strong magnetic behavior.[6] Several methods can be used to synthesize maghemite nanoparticles: sol-gel combustion process, thermal-decomposition of magnetite (Fe_3O_4) nanoparticles, solid-state synthesis, arc-discharge, mechanical grinding, laser ablation, microemulsions, co-precipitation and high temperature decomposition of organic precursors.[7-11] On the other hand, lath- and rod-shaped γ-lepidocrocite, α-goethite and β-akaganéite polymorphs of iron oxyhydroxide (FeOOH) show

* Corresponding author: hvaleria@icmpp.ro

weaker magnetic properties as compared to maghemite, but remains of considerable importance in redox-sensitive environments, being used as magnetic recording, ferrofluids, magnetic resonance imaging (MRI) fluids, abrasives or catalysts.[6] Moreover, because of the presence of the hydroxyl groups, iron oxyhydroxide shows an increased reactivity as compared to other oxide materials. Goethite was obtained by oxidation at temperatures between 20 and 70 ^{o}C,[12-13] while all processes described for the preparation of magnetite request at least one step to be performed at temperatures higher than 300 ^{o}C, Thus, owing the differences in their preparation conditions, to obtain both oxides into a single composite, new routes should be proposed.

Recently, ultrasonic-assisted processes have been a topic of intense investigation as a low-cost, simple and effective preparation method for micro or nano-structures. The well known acoustic cavitation, thermal, microjets and shockwaves phenomena occurring during ultrasonication[14,15] contribute to the formation of metal oxide particles of controllable morphology, rapid crystallization and high purity. Ultrasonication at high-intensity has been already used for the synthesis of ferromagnetic materials.[16-18] We already proved that barium titanate submicron particles and viscose/barium titanate composites can be prepared at lower duration and temperature of the thermal treatment by a process involving ultrasonnication.[19]

Herein, we present an ultrasound-based method which yields maghemite/goethite ferromagnetic composite nanoparticles in a single process. Iron sulfate was used as a source of iron ions in the presence of sodium hydroxide.

RESULTS AND DISCUSSION

1. Influence of the preparation conditions on the structure and morphology of maghemite goethite composites

Ferromagnetic maghemite-like particles were prepared by a more energy-effective method where the previously reported high temperature treatments[9-11] were replaced by ultrasonication. Ferrous sulfate known to undergo oxidation in aqueous alkaline media was used as iron source. The ultrasonication has been found much more effective for activation of the precursors, gaining thus a time-span reduction and also no need for thermal treatment. As proved below, the proposed reaction conditions allow the simultaneous preparation of maghemite/goethite composite nanoparticles.

To optimize the procedure, several attempts have been made by varying the sonication duration between 15 and 60 min. Three samples, M/G_a, M/G_b and M/G, exemplifying different preparation conditions are shown in Table 1. The resulted powder samples of colors depending on the sonication duration were characterized by FTIR, SEM, TEM and X-ray diffraction to follow the influence of the preparation conditions on the conversion of the reagents into maghemite/goethite composite. Finally, the ultrasound time-span was established at 60 minutes that represent the lower limit for the full conversion of the reagents to the desired ferromagnetic nanoparticles.

FT-IR analysis

The structures of maghemite/goethite composite powder (M/G) and of the partially converted samples (M/G_a and M/G_b) were first assessed through infrared spectroscopy. The assignment of the characteristic bands (Table 2) was made based on literature information[6,20-24] and in correlation with XRD analysis.

As one may see from data in Table 2, for M/G_a sample, most of the vibrations are specific to sulfate groups. Goethite was also detected by the very sharp band located at 879 cm^{-1}, while a very large and intense absorption band attributed to the stretching of different OH groups and to water appeared between 2890 and 3887 cm^{-1}. The characteristic absorptions of M/G_a sample clearly indicate that the ultrasonication for 15 minutes (about 30 kJ dissipated) does not provide the energy needed for the development of maghemite crystallites and for full transformation of the iron sulfate precursor. M/G_b sample obtained at 30 minutes of sonication is characterized by only a medium intensity band at 870 cm^{-1} attributed to goethite, while sulfate bands are still present and the large OH band was replaced by shorter and more resolved bands located at 2903 and at wave numbers higher than 3000 cm^{-1}. Moreover a strong modification of the spectral absorption in the region 700-500 cm^{-1} was noticed that could be attributed to the superposed maghemite and sulfate bands. By the contrary, the spectrum of M/G sample showed only characteristic bands for maghemite and goethite. The band at 579 cm^{-1} of a higher intensity, attributed to ν(Fe-O) (intrinsic stretching) indicates the formation of γ-Fe_2O_3 as

one of the phase of the composite. The bands at 795 and 885 cm^{-1} (deformational modes of hydroxyl groups, δ-OH out of plane and in plane), typical for goethite are well-defined and sharp indicating also the presence of goethite. However, adsorbed water (1628 cm^{-1}) and SO_4^{2-} (light traces) are also detectable in the spectrum of M/G sample. One should mention that sulfate traces around 1250-1450 cm^{-1} are present in many synthesis where $FeSO_4$ is the iron source.

Table 1

Composite samples prepared under different sonication durations

Sample Code	Ultrasonic time-span [minutes]	Energy dissipated [kJ]	Conversion of the reagents	Powder product color
M/G_a	15	30,5	Incomplete transformation	reddish brown
M/G_b	30	59	Incomplete transformation	reddish-yellow brown
M/G	60	109	Full transformation	dark brown

Table 2

Interpretation of spectral bands in FTIR spectra

Sample	Band Position [cm^{-1}]	Vibration Mode, Interpretation
M/G_a	420, 555, 636, 701	ν_{ab} SO_4: asymmetric bending of SO_4 group[20]
	783	δ-OH out of plane: goethite[6 p.144, 13]
	809	ν_{as} SO_4 asymmetric stretching of SO_4 group[20]
	879	δ(OH) in plane: goethite[6 p.144, 13]
	970	ν_{ss} (SO_4): symmetric stretching of sulfates[21]
	1156	$\nu_3(SO_4^{2-})$: sulfate absorptions[22,23]
	1435	$\nu(SO_4)$[6,22]
	1642	δ(OH): absorbed water[6,22]
	2790 - 3887, 2861, 2950	OH stretching: surface hydroxyl groups and H_2O[6 p.143-144]
M-G_b	519, 687	ν_{ab} SO_4: asymmetric bending of SO_4 group[20]
	870	δ(OH) in plane: goethite[6 p.144,13]
	972	ν_{as} SO_4 asymmetric stretching of SO_4 group[20]
	1157	SO_4: adsorbed sulfate groups[22,23]
	1412, 1445	$\nu(SO_4)$[6,22]
	1665	δ(OH): absorbed water[6,22]
	2903, 3057	H-OH: intramolecular frequencies[24]
	3323, 3441, 3626, 3543, 3859	OH stretching: surface hydroxyl groups and H_2O[6 p.143-144]
M-G	399, 453	τ_{OH} : goethite[6 p.143]
	579	ν(Fe-O): intrinsic stretching: maghemite[6 p.146]
	795, 885	δ-OH out of plane and in plabe, repectively: goethite[6 p.144, 13]
	1047, 1117	Fe-O asymmetric stretching: goethite[24]
	1259, 1369, 1429	$\nu(SO_4)$: light traces, from synthesis[6,22]
	1628	δ(OH): absorbed water[6,22]
	2183, 2361	possible CO_2 from measuring conditions, light traces
	2849	ν(OH): goethite or lepidocrocite[6 p.143-144]
	2920	H-OH: intramolecular frequencies[24]
	3152	ν(OH): bulk hydroxyl stretching in goethite structures[6 p.143]
	3435, 3667, 3738, 3842, 3858, 3871, 3890	OH stretching: surface hydroxyl groups and H_2O [6 p.143-144]

Electron microscopy

The structures and dimensions of the prepared samples were further analyzed by SEM and TEM analysis. Fig. 1 shows the SEM micrographs of M/G_a, M/G_b and M/G samples.

The SEM micrograph for M/G_a shows a porous surface built by large agglomeration of not individualized particles indicating that important inter-particle interactions are characteristic for this system. The particles become more individualized and the dimensions decreased as the span-time of sonication increases. Thus, polydisperse micrometric particles can be observed for M/G_b, while the size of the M/G particles became very small. As the

SEM image of M/G composite is not concluding, the sample was analyzed by TEM (Fig. 3). Maghemite particles of approximately spherical shape and different sizes, generally less than 100 nm, some of them being less than 50 nm are surrounding the goethite acicular formations with lengths around or higher than 100 nm and diameters of around 10 nm. The TEM images clearly indicate the formation of maghemite/ goethite composite for the sample prepared under sonication for 60 minutes.

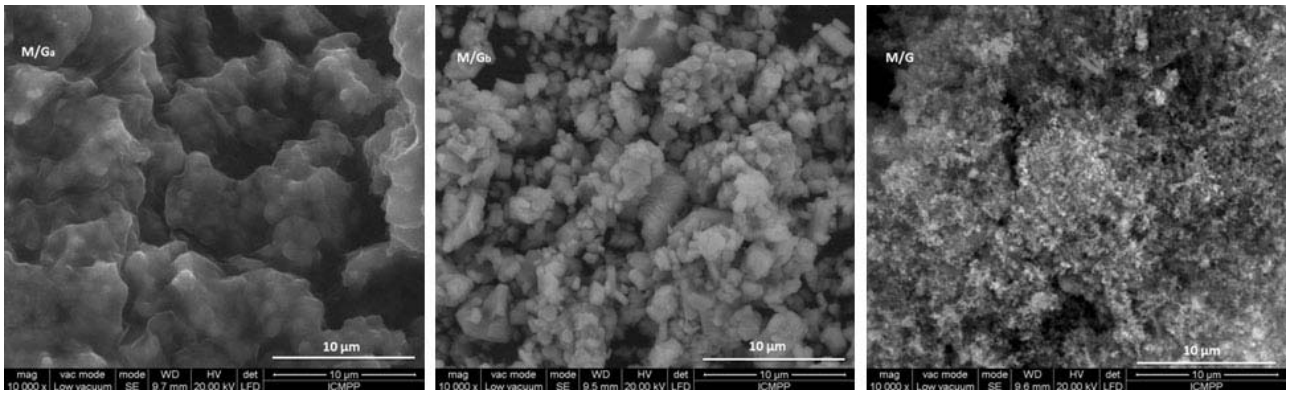

Fig. 1 – SEM micrographs of M/G_a, M/G_b and M/G samples.

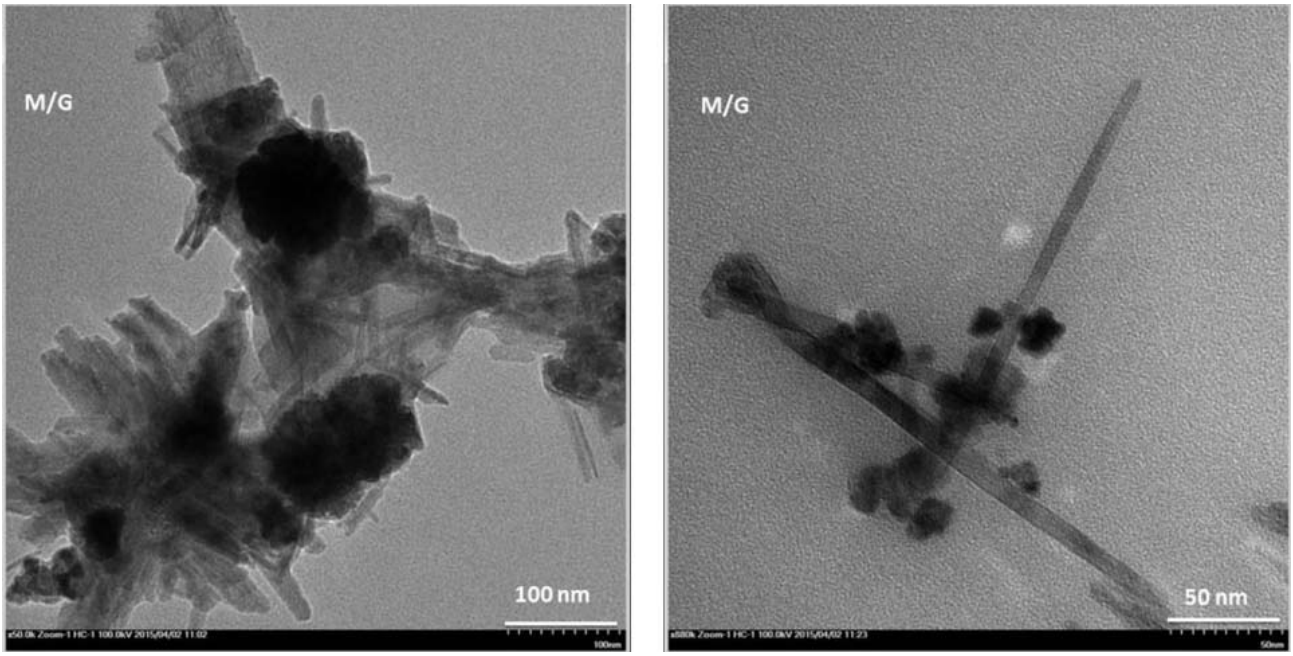

Fig. 2 – TEM images of M/G composite.

X-Ray diffraction

The recorded XRD pattern of M/G sample is shown in Fig. 3. All the peaks observed in the XRD profile correspond to maghemite (according to JCPDS card number 39-1346) and goethite (according to JCPDS card number 03-0251). The diffraction angles and planes as well as the interplanar distances (calculated with Bragg equation ($2d\sin\theta = n\lambda$)) are given in Table 3. Thus, the XRD analysis is in strong correlation with the IR spectroscopy and TEM observations and confirms the formation of maghemite/goethite composite. These results demonstrate that ultrasonication of the iron sulfate in basic medium of sodium hydroxide allowed simultaneous formation of maghemite and goethite structures at room temperature.

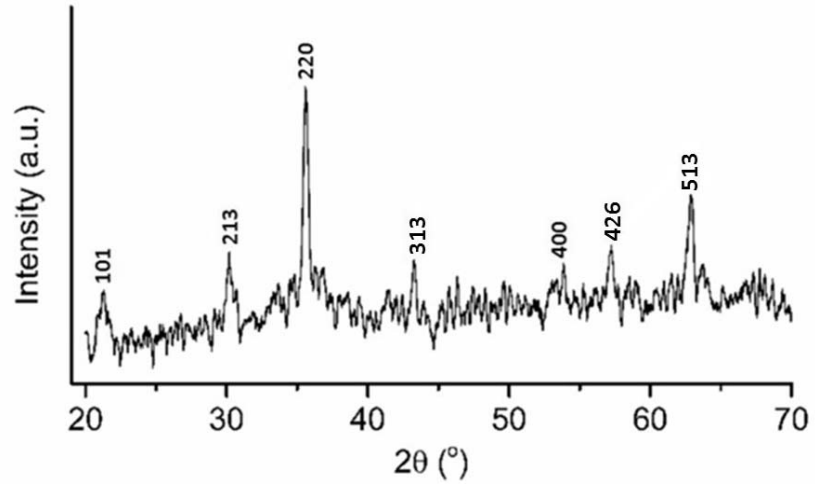

Fig. 3 – Diffraction pattern of M/G composite.

Table 3

Diffraction angles, diffraction planes (Miller planes) and interplanar distances

2θ [°]	Assignment	Miller index	Interplanar Distances [nm]
21.26	Goethite	101	0,41
30.22	Maghemite	213	0,34
35.62	Maghemite	220	0,29
43.24	Maghemite	313	0,25
53.90	Maghemite	400	0,20
57.20	Maghemite	426	0,17
62.94	Maghemite	513	0,16

2. Mechanism of simultaneous synthesis of maghemite/goethite composite

The following mechanism of the one-pot preparation of maghemite/goethite composites under ultrasonication of iron sulphate-sodium hydroxide mixed solutions in air could be envisaged by correlating the information obtained from IR, SEM, TEM and XRD analysis of samples obtained in different conditions (Scheme 1). Ferrous hydroxide is first obtained through the reaction between iron sulfate and sodium hydroxide. In the presence of oxygen and under ultrasonication, this one is oxidized to iron oxide hydroxide that further undergoes the dehydration reaction resulting in the formation of maghemite. Under ultrasonication for 60 minutes only partial transformation of goethite into maghemite is achieved. Thus, the resulted powder contains both iron compounds.

Transformation of iron sulfate in iron oxyhydroxide

$$FeSO_4 + 2\ NaOH \rightarrow Fe(OH)_2 + Na_2SO_4 + H_2O$$

$$Fe(OH)_2 + 1/2O_2 \rightarrow FeOOH\ (\text{lepidocrocite or goethite}) + H_2O$$

Partial dehydration of iron oxyhydroxide to maghemite

$$2FeOOH \rightarrow \gamma\text{-}Fe_2O_3\ (\text{maghemite}) + H_2O$$

Scheme 1 – Chemistry of simultaneous preparation of maghemite/ goethite composites under ultrasonication at room temperature.

3. Magnetic properties

The magnetic properties of the as-prepared maghemite/goethite nanocomposite (M/G) were monitored by measuring the hysteresis loops (magnetization curves) at different temperatures (10, 20, 30, 40, 50, 100, 200 and 300 K) (Fig. 4). The sample shows narrow hysteresis loops. The saturation values of the magnetic moment are of 0.45 emu at 300 K and 0.57 emu at 10 K (for a mass of 7.545 mg analyzed).

The dependence of the magnetization on temperature was measured using zero field cooling (ZFC) and field cooling (FC) procedures (Fig. 5), between 10 and 250 K, at decrement and increment rates of 2 K/min. On this temperature interval, ZFC and FC curves show a characteristic feature of ferromagnetic materials, i.e., a slow growth of the magnetic moment at low temperatures for ZFC and a much smaller variation for FC on the entire temperature range. No blocking temperature, specific to paramagnetic materials, but only a transition temperature at 144 K (-129 °C) was observed. Above this temperature an acceleration of the magnetization was noticed.

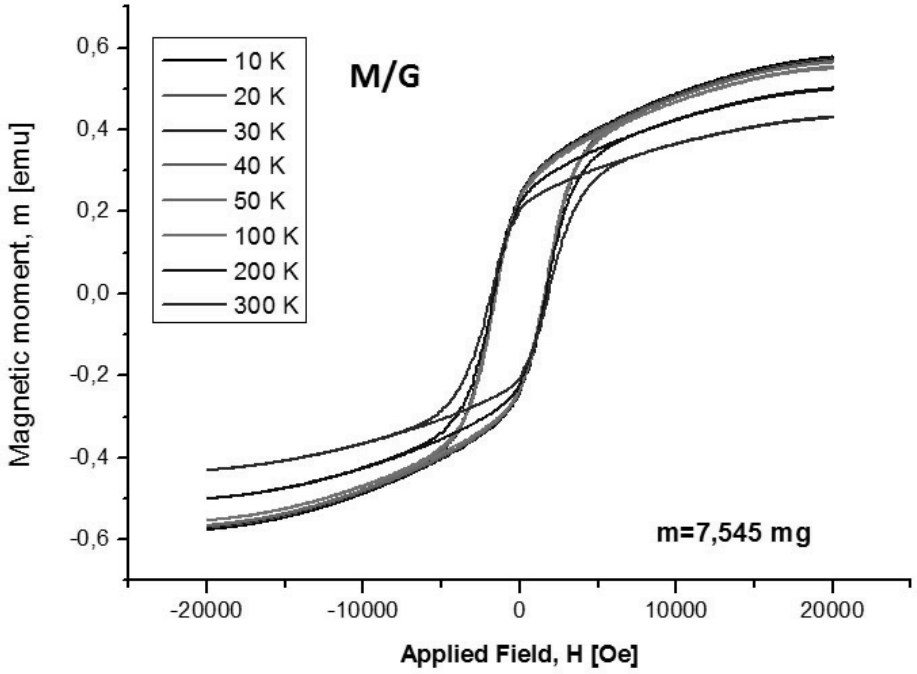

Fig. 4 – Evolution of the magnetic hysteresis curves for M/G composites as a function of temperature.

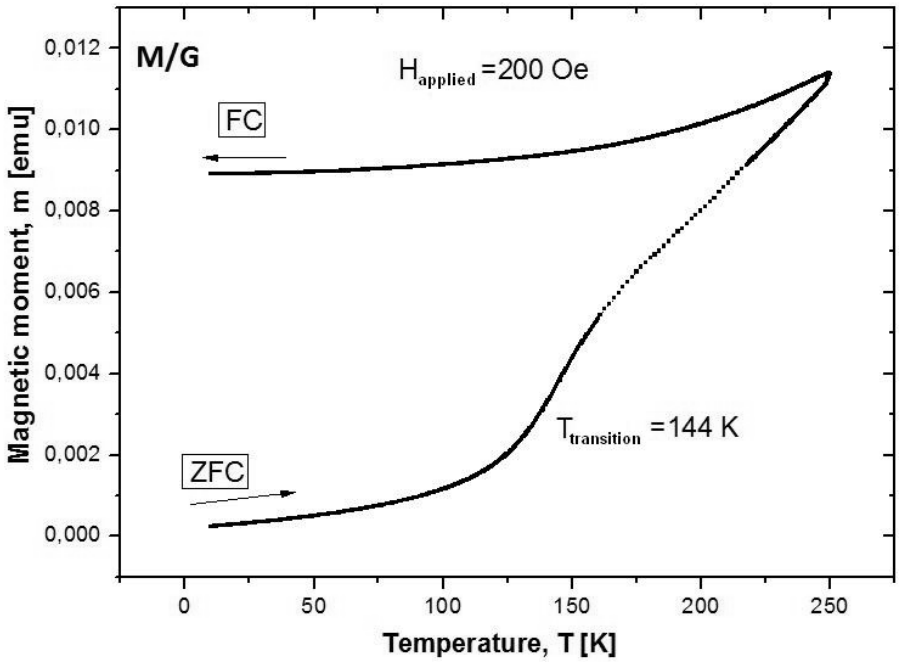

Fig. 5 – Thermomagnetic curves (temperature dependence of magnetization measured using standard zero field cooling (ZFC) and field cooling (FC) procedure) for M/G.

The variation of the coercive field and of M_r/M_S ratio (M_r: remanent magnetization, M_s: saturation magnetization) with temperature is shown in Fig. 6. Ms, Mr and Hc are determined from the hysteresis curves presented in Fig. 4, where Ms is the saturation value of the magnetic moment, Mr is the value of the magnetic moment at H = 0 and Hc is the coercive field value, i.e. the field at which the magnetization is passing through 0. M_S was found to vary from 59.6 emu/g at room temperature (~300 K) to 75.5 emu/g at low temperature (10 K), lower as compared to 84 emu/g, a maximum value found for pure maghemite at room temperature,[25] but higher than other early reported values. For example, Aliahmad prepared γ-Fe_2O_3 nanoparticles by

thermal-decomposition of Fe_3O_4 that showed Ms of 31 emu/g (room temperatures),[9] while Layek *et al.*[10] and Kluchova *et al.*[11] presented Ms values of 13.3 emu/g and 53.18 emu/g, respectively, for maghemite nanoparticles synthesized by chemical co-precipitation technique. The saturation magnetization value obtained for maghemite/ goethite composite could be ascribed to surface effects arising from broken symmetry and also to a high degree of maghemite/goethite interparticle interactions.

Both the coercive field and M_r/M_S ratio are decreasing with the increase of temperature (the coercive field is 7000 Oe at 10 K and 1000 Oe at 300 K, while M_r/M_S is 0.87 at 10 K and 0.41 at 300 K, respectively), a normal behavior for a ferromagnetic material (the magnetic properties are enhanced at low temperatures).

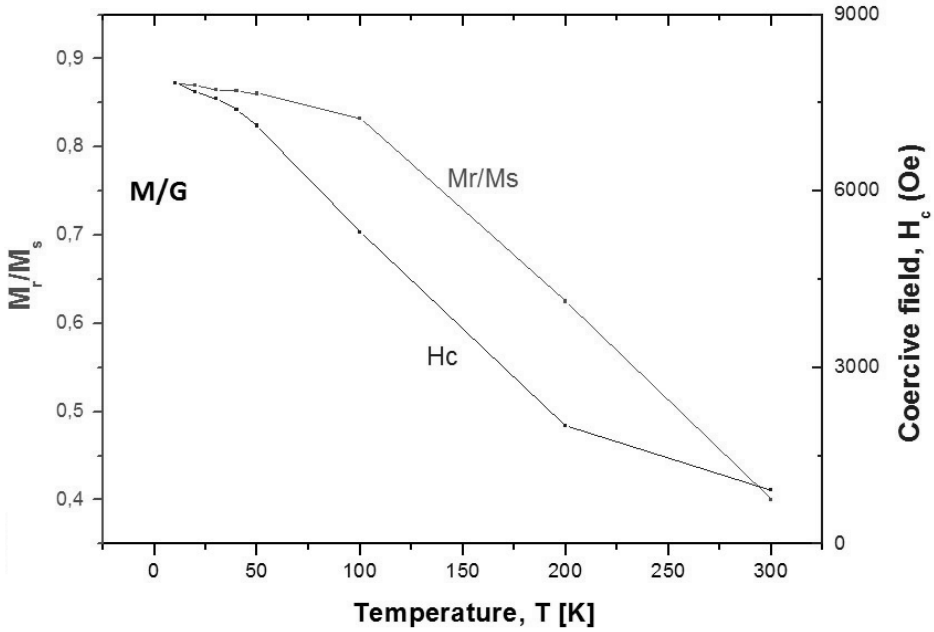

Fig. 6 – Dependence of remanent magnetization/saturation magnetization ratio (Mr/Ms) and of coercive field on temperature for M/G composite sample.

EXPERIMENTAL

Materials

Iron sulfate heptahydrate ($FeSO_4 \cdot 7H_2O$: Sigma-Aldrich, 99% purity), sodium hydroxyde pellets (Merck, 99% purity) and Milli-Q ultrapure distilled water (our laboratory) were used without further purification.

2. Preparation of maghemite/goethite nanoparticles (M/G)

M/G nanoparticles were prepared through a multistep procedure as follows. First, $FeSO_4/H_2O$ 1/2 w/w and $NaOH/H_2O$ 1/4 w/w solutions were prepared in ultrapure water and mixed (1/1 w/w ratio) in a ultrasonic bath of a Sonics Vibracell ultrasound generator (750W nominal electric power, 20 kHz ultrasound frequencies; amplitude, 50% of the maximum intensity) equipped with a display for the delivered energy and a sensor for temperature. A cylindrical ultrasonic bath was chosen (100 ml Schott-Duran Berzelius beaker) as previously described by Capelo *et al.*[26]. The amounts of iron sulfate and of sodium hydroxide solutions were chosen based on the technical requirements of ultrasonic probe generator (the water level does not exceed 40% of the probe length). The beaker was placed on an ice bath and the temperature was rapidly increasing during sonication up to 25 ^oC. The energy dissipated in the ultrasonic bath was 30, 59 and 109 kJ after sonication for 15, 30 and 60 minutes, respectively. The samples were than centrifuged, washed with Milli-Q water, centrifuged again and dried in a Trade Raypa vacuum oven for 24 h at 40 °C to obtain powder samples of colors depending on the ultrasonication duration.

3. Characterization

The structure of the maghemite/goethite ferromagnetic composite samples was investigated by FTIR spectroscopy on potassium bromide pellets on a Bruker Vertex 70 Spectrometer. An ESEM Quanta 200 electronic deflection microscope and a Hitachi HT 7700 electron transmission microscope were used to visualize the surface morphologies. The crystallization patterns were obtained on a Bruker Advance D8 X-ray diffractometer (λ: 0.15405 nm - the wavelength of Cu Kα1 radiation, 2θ from 5 to 100 degrees-angular region). The magnetic measurements (magnetization curves, magnetization dependence on temperature, M_r/M_S, and coercive field dependence on temperature) were performed on a Quantum Design-PPMSQD-9 vibrating sample magnetometer (-20÷20 kOe range for applied magnetic field); the magnetization dependence on temperature was followed by using standard zero field cooling (ZFC) and field cooling (FC) procedures between 10 and 250 K for the applied field of 200 Oe).

CONCLUSION

A ferromagnetic and hydroxyl functionalized maghemite/goethite composite has been prepared at room temperature through a chemical precipitation process and ultrasonication in a basic medium. XRD and FTIR results indicated the formation of maghemite and goethite. Particle agglomerates with average diameter less than 100 nm (maghemite) and acicular particles (goethite) with lengths higher than 100 nm and diameters of about 10 nm were observed by TEM analysis. VSM studies have revealed ferromagnetic character of the composite with a saturation magnetization (M_S) varying from 59.6 emu/g (room temperature) to 75.5 emu/g (low temperature). The established process parameters allowed well defined γ-Fe_2O_3/α-FeOOH nanometric particles with appropriate properties for applications as ferromagnetic materials. Moreover, the maghemite/goethite ferromagnetic composite which combines the properties of both precursors could be of interest in the development of new polymeric composites (higher magnetization and hydroxyl functional groups able to mutually interact with those of the polymer matrix).

Acknowledgement: The authors acknowledge the support of the Project nr. 276/2014, PARTNERSHIPS Program of MEN-UEFISCDI.

REFERENCES

1. B. Weglinski, *Reviews on P/M and Physical Ceramics*, **1990**, *4*, 79-154.
2. J. Chumming and L. Xiangqin, *J. Solid State Electrochem*., **2009**, *13*, 1273-1278.
3. T. Y. Liu, S. H. Hu, D. M. Liu, S. Y. Chen and I. W. Chen, *Nano Today*, **2009**, 4, 52-65.
4. Y. Xiang, J. Wang, S. H. Hussain and G. P. Krestin, *Eur Radiol*, **2001**, *11*, 2319–2331.
5. R. Weissleder, A. Moore, U. Mahmood, R. Bhorade, H. Benveniste, E. A. Chiocca and J. P. Basilion, *Nat. Med.*, **2000**, *6*, 351-355.
6. R. M. Cornell, U. Schwertmann, "The Iron Oxides: Structure, Properties, Reactions, Occurrences and Uses", second edition, **2003**, WILEY-VCH Verlag GmbH & Co. KGaA, Weinheim, p. 87-91.
7. C. Cannas, A. Ardu, D. Niznansky, D Peddis, G. Piccaluga and A. Musinu, *J. Sol-Gel Sci. Technol.*, **2011**, *60*, 266-274.
8. J. Hu, I. M. C. Lo and G. H. Chen, *Water Res*., **2005**, *39*, 4528–4536.
9. M. Aliahmad, N. Nasiri Moghaddam, *Mater. Sci. - Poland*, **2013**, *31*, 264-268.
10. S. Layek, A. Pandey, A. Pandey and H. C. Verma1, *Int. J. Eng. Sci. Technol.*, **2010**, *2*(8), 33-39.
11. K. Kluchova, R. Zboril, J. Tucek, M. Pecova, L. Zajoncova, I. Safarik, M. Mashlan, I. Markova, D. Jancik, M. Sebela, H. Bartonkova, V. Bellesi, P. Novak and D.Petridis, *Biomaterials*, **2009**, *30*, 2855-2863.
12. U. Schwertmann and R. M. Cornell, "Iron Oxides in the Laboratory: Preparation and Characterization", second edition, WILEY-VCH, Weinheim, New York, Chichester, Brisbane, Singapore, Toronto, 2000, p. 67-91.
13. G. Montes-Hernandez, P. Beck, F. Renard, E. Quirico, B. Lanson, R. Chiriac and N. Findling, *Cryst. Growth Des.*, **2011**, *11*, 2264-2272.
14. K. S. Suslick, Y. Didenko, M. M. Fang, T. Hyeon, K. J. Kolbeck, W. B. McNamara III, M. M. Mdleleni and M. Wong, *Phil. Trans. R. Soc. London*, **1999**, *A 357*, 335-353.
15. H. M. Santos, C. Lodeiro, and J. L. Capelo-Martinez, in J.-L. Capelo-Martínez, "Ultrasound in Chemistry: Analytical Applications", WILEY-VCH Verlag GmbH & Co. KGaA, Weinheim, 2009, p. 1-15.
16. M. J. Smith, V. H.B. Ho, N. J. Darton and N. K. H. Slater, *Ultrasound Med. Biol*., **2009**, *35*, 1010-1014.
17. L. F. Rychkov, M. S. Goronchko, A. M. Nesterenko and Z. M. Yakovleva*, Sov. Min. Sci.,* **1982**, *18*, 352-354.
18. R. Vijaya Kumar, Y. Koltipin, X. N. Xu, Y. Yeshurun, A. Gedanken and I. Felner, *J. Appl. Phys*., **2001**, *89*, 6324-6328.
19. R. Rotaru, C. Peptu, V. Harabagiu, *Cell. Chem. Technol.*, **2016**, *50*, 621-628.
20. J. L. Capelo, M. M. Galesio, G. M. Felisberto, C. Vaz and J. C. Pessoa, *Talanta*, **2005**, *66*, 1272–1280.
21. N. Salami and F.A. Adekola, *Bull. Chem. Soc. Ethiop*., **2002**, *16*, 1-7.
22. A. Periasamy, S. Muruganand and M.Palaniswamy, *Rasayan J. Chem.*, **2009**, *2*, 981-989.
23. M. Gotic and S. Music, *J. Mol. Struct*., **2007**, *834* (*836*), 445–453.
24. D. Peak, R. G. Ford and D. L. Sparks, *J. Colloid. Interface Sci.*, **1999**, *218*, 289–299.
25. Z. C. Ling and A. Wang, *Icarus*, **2010**, *209*, 422-433.
26. J. L. Dormann, D. Fiorani and E. Tronc, *Adv. Chem. Phys.*, **1997**, *98*, 283–294.